NeuroImage 245 (2021) 118708

Contents lists available at ScienceDirect

NeuroImage

journal homepage: www.elsevier.com/locate/neuroimage

Recording brain responses to TMS of primary motor cortex by EEG – utility of an optimized sham procedure

Pedro C. Gordon[a,b], D. Blair Jovellar[a,b], YuFei Song[a,b], Christoph Zrenner[a,b], Paolo Belardinelli[a,b,c], Hartwig Roman Siebner[d,e,f], Ulf Ziemann[a,b,*]

[a] Department of Neurology & Stroke, University of Tübingen, Hoppe-Seyler-Straße 3, Tübingen 72076, Germany
[b] Hertie Institute for Clinical Brain Research, University of Tübingen, Germany
[c] CIMeC, Center for Mind/Brain Sciences, University of Trento, Italy
[d] Danish Research Centre for Magnetic Resonance, Centre for Functional and Diagnostic Imaging and Research, Copenhagen University Hospital – Amager and Hvidovre, Copenhagen, Denmark
[e] Department of Clinical Medicine, Faculty of Health and Medical Sciences, University of Copenhagen, Denmark
[f] Department of Neurology, Copenhagen University Hospital – Bispebjerg and Fredriksberg, Copenhagen, Denmark

ARTICLE INFO

Keywords:
Transcranial magnetic stimulation
Electroencephalography
TMS-EEG
Sham stimulation
Peripherally evoked potentials

ABSTRACT

Introduction: Electroencephalography (EEG) is increasingly used to investigate brain responses to transcranial magnetic stimulation (TMS). A relevant issue is that TMS is associated with considerable auditory and somatosensory stimulation, causing peripherally evoked potentials (PEPs) in the EEG, which contaminate the direct cortical responses to TMS (TEPs). All previous attempts to control for PEPs suffer from significant limitations.

Objective/Hypothesis: To design an optimized sham procedure to control all sensory input generated by subthreshold real TMS targeting the hand area of the primary motor cortex (M1), enabling reliable separation of TEPs from PEPs.

Methods: In 23 healthy (16 female) subjects, we recorded EEG activity evoked by an optimized sham TMS condition which masks and matches auditory and somatosensory co-stimulation during the real TMS condition: auditory control was achieved by noise masking and by using a second TMS coil that was placed on top of the real TMS coil and produced a calibrated sound pressure level. Somatosensory control was obtained by electric stimulation (ES) of the scalp with intensities sufficient to saturate somatosensory input. ES was applied in both the sham and real TMS conditions. Perception of auditory and somatosensory inputs in the sham and real TMS conditions were compared by psychophysical testing. Transcranially evoked EEG signal changes were identified by subtraction of EEG activity in the sham condition from EEG activity in the real TMS condition.

Results: Perception of auditory and somatosensory inputs in the sham vs. real TMS conditions was comparable. Both sham and real TMS evoked a series of similar EEG signal deflections and induced broadband power increase in oscillatory activity. Notably, the present procedure revealed EEG potentials and a transient increase in beta band power at the site of stimulation that were only present in the real TMS condition.

Discussion: The results validate the effectiveness of our optimized sham approach. Despite the presence of typical responses attributable to sensory input, the procedure provided evidence for direct cortical activation by subthreshold TMS of M1. The findings are relevant for future TMS-EEG experiments that aim at measuring regional brain target engagement controlled by an optimized sham procedure.

1. Introduction

The combined use of electroencephalography (EEG) and transcranial magnetic stimulation (TMS) allows the probing of immediate cortical responses to brain stimulation in a safe and non-invasive approach, expanding the available tools for understanding human neurophysiology. TMS-EEG can potentially be employed in the investigation of local neuronal excitability of any cortical region targeted by TMS, and alterations in cortical responses associated with drugs acting on the central nervous system, neuromodulatory interventions or neuropsychiatric disorders (Ilmoniemi et al., 1997; Esser et al., 2006; Rogasch and Fitzgerald, 2013; Tremblay et al., 2019). Despite its potentials, the technique

* Corresponding author at: Department of Neurology & Stroke, University of Tübingen, Hoppe-Seyler-Straße 3, Tübingen 72076, Germany.
E-mail address: ulf.ziemann@uni-tuebingen.de (U. Ziemann).

https://doi.org/10.1016/j.neuroimage.2021.118708.
Received 23 June 2021; Received in revised form 31 October 2021; Accepted 2 November 2021
Available online 4 November 2021.

is not free of caveats. One significant issue is that the EEG responses to TMS are not limited to transcranial cortical activation (the so called TMS evoked potentials – TEPs), but in addition reflect activation by multisensory inputs also caused by TMS. These peripherally evoked potentials (PEPs) are cortical responses that follow the sensory (auditory and somatosensory) input, and present as EEG deflections of considerable amplitude starting at around 100 ms (Ilmoniemi and Kicic, 2010). Consequently, PEPs are superimposed to TEPs, significantly hindering TMS-EEG data interpretation (Ilmoniemi and Kicic, 2010). Several attempts have been proposed to overcome this limitation. However, most have failed to consistently control for sensory inputs from real TMS. Also, attempts to reproduce the PEPs by sham procedures were limited by failure to generate sensory inputs comparable to those produced by real TMS (Belardinelli et al., 2019; Conde et al., 2019; Siebner et al., 2019).

The contamination of TMS-EEG data with PEPs has been identified since the implementation of the technique, with auditory input found responsible for significant evoked potentials in TMS-EEG experiments (Nikouline et al., 1999; Paus et al., 2001). TMS-related auditory input involves a high-pitched "click" sound generated during coil discharge—a result of the brief coil vibration as the electric current runs through its windings—which is clearly audible by subjects (Nikouline et al., 1999), and sound pressure level can significantly exceed 100 dB (Counter and Borg, 1992; Koponen et al., 2020). It has been suggested that the auditory PEP accounts for most of the undesired indirect cortical activation in TMS-EEG experiments, stressing the importance of a proper control method to allow experiments to retrieve the true TEPs in the EEG signal (Paus et al., 2001; Ilmoniemi and Kicic, 2010; Rocchi et al., 2021). The use of earplugs to muffle significantly attenuates the sound pressure level in the ear canal (Counter and Borg, 1992), but was found to be largely insufficient in suppressing the auditory PEP (Nikouline et al., 1999; ter Braack et al., 2015). Alternatively, the use of masking noise has been suggested, specifically one that contains the same frequency spectrum distribution as the TMS click (Massimini et al., 2005), a procedure which was found very effective in suppressing the auditory PEP (Gosseries et al., 2015; ter Braack et al., 2015). Another proposed approach is the use of a sham condition in which an equivalent click sound is generated by a sham procedure, usually a sham coil, or a real coil placed away from the cortex. Studies that used this procedure aimed to compare the signals from the sham and real TMS conditions, as concurrent responses in both signals would indicate the PEP, and the remaining response in the real TMS condition can then be attributed to the true direct cortical activation by TMS (Casali et al., 2010; Herring et al., 2015; Du et al., 2017; Gordon et al., 2018; Conde et al., 2019).

In addition to the auditory input, somatosensory inputs from TMS were also found to contribute to the PEP in TMS-EEG experiments. The electric field induced by the time-varying magnetic field of TMS extends inevitably through extracranial tissue and activates trigeminal axons and scalp muscles. The trigeminal somatosensory input and reafferents from the muscle twitches result in somatosensory responses in the EEG signal (Herring et al., 2015; Conde et al., 2019). Proposed solutions involve the use of a sham condition that would reproduce the somatosensory input generated by TMS, analogous to the principle behind the auditory sham control. Previous studies proposed electric stimulation with electrodes placed on the same scalp region as the TMS target (Rossi et al., 2007; Mennemeier et al., 2009), which would deliver a similar scalp sensation, theoretically generating PEPs equivalent to those in the real TMS condition.

Despite these proposed solutions, only few studies attempted to employ these control methods. It is unclear to what extent the results obtained by these uncontrolled TMS-EEG studies represent EEG responses from direct cortical activation, or rather non-specific PEPs. Moreover, critical reports have identified that even those studies that attempted to employ these methods have failed to design a realistic sham control condition that properly matched the multisensory inputs of real TMS (Belardinelli et al., 2019; Siebner et al., 2019). So far, no consensus has been reached on how to create an ideal sham procedure in TMS-EEG studies, resulting in a critical view on the validity and interpretability of current TMS-EEG studies.

Here, we aim to design and test an optimized sham procedure for TMS-EEG experiments that will overcome the limitations presented by the previously proposed sham procedures. Specifically, the optimized sham would deliver the same multisensory stimuli as real TMS, meaning that their perception is identical in psychophysical testing, and PEPs are equivalent between sham and real TMS. By meeting these conditions, a comparison between the signals from the sham and the real TMS conditions should imply that any differences are largely to be attributed to direct cortical activation by TMS, thus revealing TEPs in a specific manner. The objectives of the present study were: (1) To design such optimized sham TMS condition; (2) to test the perception of the sensory inputs from the optimized sham TMS and compare them with the real TMS condition; and (3) to compare the EEG responses in the optimized sham vs. real TMS conditions.

2. Methods

2.1. Subjects and design

The experiment involved right-handed healthy volunteers that participated in a single session. Inclusion criteria were age between 18 and 50 years and competency to provide informed consent to participate in the study. Exclusion criteria were presence or history of psychiatric or neurological diseases, intake of drugs acting on central nervous system, presence or history of alcohol or illicit drugs abuse, and current pregnancy. Subjects with resting motor threshold (RMT) > 60% of the maximum stimulator output (MSO) were also excluded, as higher intensities would involve higher auditory input and compromise the sham procedure (see section *Optimized sham TMS design*).

A total of 23 (16 female) subjects was included in this study, with a mean age of 25 years (SD ± 4.4). All subjects provided written informed consent prior to participation. The study was approved by the ethics committee of the medical faculty of the University of Tübingen (456/2019BO2) and conformed to the latest version of the Declaration of Helsinki.

2.2. Experimental set-up

The experiment was conducted in a quiet room with the subjects sitting comfortably on a reclined chair, instructed to keep their eyes opened during the measurements. Prior to the TMS-EEG session, all subjects underwent magnetic resonance imaging (MRI) using a 3T Siemens PRISMA scanner with T1-weighted anatomical sequences. MRI was required for proper positioning of the TMS coil with respect to the individual's brain anatomy, using a neuronavigation system (Localite GmbH, Sankt Augustin, Germany), and also for the EEG forward model and source reconstruction, explained below.

Scalp EEG was recorded from a TMS compatible 64-channel Ag/AgCl sintered ring electrode cap (EasyCap GmbH, Germany). Additionally, surface EMG was recorded through bipolar EMG adhesive hydrogel electrodes (Kendall, Covidien) over the abductor pollicis brevis (APB) and first dorsal interosseus (FDI) muscles of the right hand in a bipolar belly-tendon montage (5 kHz sampling rate, 0.16 Hz–1.25 kHz bandpass filter). EMG was used for determination of RMT with standard methods (Groppa et al., 2012), using the individual MRI and neuronavigation to guide the coil position and maintain its orientation perpendicular to the precentral sulcus, and then selecting the cortical target that elicited highest motor evoked potentials (MEP) amplitudes as the *hot-spot*. EMG was also recorded for detection of possible MEPs during the TMS-EEG measurements. TMS was delivered using a figure-of-eight coil (external diameter of each wing 90 mm) connected to a Magstim 200^2 magnetic stimulator (Magstim Company Ltd., UK) with a monophasic current waveform. Two identical stimulators and coils were used in this

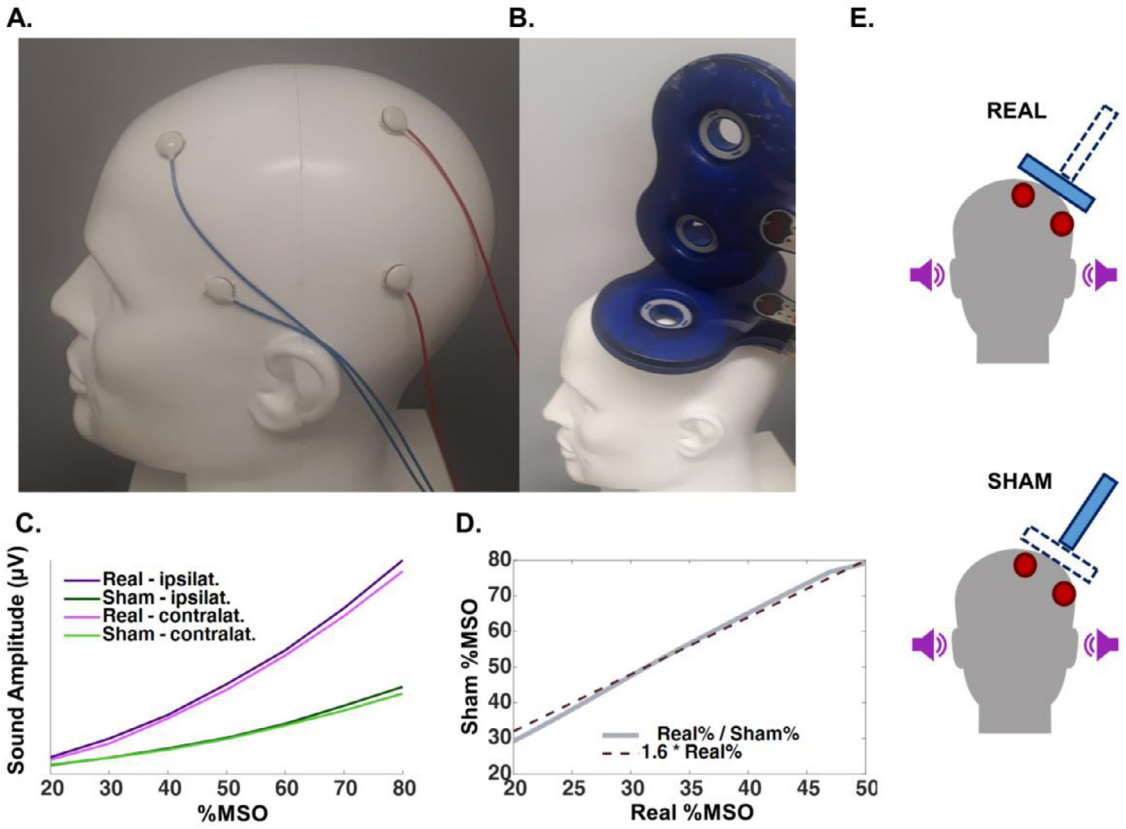

Fig. 1. **A.** Head model illustrating the positioning of the electrodes for electric stimulation, 2 electrodes of the same polarity at FFT9h and AFF5h (blue cables), and 2 electrodes of the opposite polarity at CPP3h and TPP7h (red cables). Polarities switched after each pulse. **B.** Illustration of the positioning of the real TMS coil (in contact with the head) and sham TMS coil (above the real coil and tilted by 90 °). **C.** Sound amplitude of the coil click summed over 50 ms, measured by microphones in the ear canals ipsilateral and contralateral to real and sham TMS. **D.** Sound amplitude relation between the real and the sham TMS conditions according to TMS intensity (%MSO), which follows approximately a linear function, with real%MSO = 1.6 x sham%MSO. **E.** Depiction of the real and sham TMS set-up, both showing delivery of masking noise (purple sound-icons) and electric stimulation (red electrodes), but differ with respect of the TMS coil activated, as real TMS involved discharging the coil tangentially on the scalp, but sham TMS the coil on top of the real TMS coil and tilted 90 ° with respect to the scalp (blue rectangles) (For interpretation of the references to color in this figure legend, the reader is referred to the web version of this article).

experiment, one for the real TMS condition and the other for the sham TMS condition. Finally, electric stimulation (ES) of the scalp was delivered by a Digitimer DS7A (Digitimer Ltd. UK).

TMS targeted the hand area of left primary motor cortex (M1), with coil orientation perpendicular to the central sulcus, as informed by the neuronavigation system. The intensity used for the real TMS condition was 90% RMT. This subthreshold intensity was chosen to avoid somatosensory input via re-afferent feedback from MEP-related muscle twitches (Paus et al., 2001; Fecchio et al., 2017), while this intensity is sufficient to produce TEPs (Komssi and Kahkonen, 2006; Fecchio et al., 2017)

2.3. Optimized sham TMS design

As described in the Introduction, the two major sources of sensory input elicited by TMS are auditory and somatosensory. To control for the auditory input, we applied masking noise of the same spectral distribution as the coil click during the measurements (Massimini et al., 2005). Despite the reported success of this procedure in suppressing auditory PEPs, there is evidence that the procedure is not sufficient to completely cancel the auditory input (Conde et al., 2019). We share this experience in our laboratory, as some subjects can still hear the TMS click despite application of masking noise at maximum tolerable intensity. To account for this potential limitation, we added another control method in the form of a sham TMS procedure, involving an identical TMS stimulator and coil as for the real TMS condition, but having the coil tilted at a 90-degree angle with respect to the scalp and positioned on top of the real TMS coil, so that the sham coil would not induce current in the cortex (Fig. 1B). However, the difference in the distance from the source of the auditory stimulus to the ear will lead to differences in sound pressure level at the ear, if both coils are discharged with identical stimulus intensity. To account for this, we performed measurements using a head model and 3 mm microphones (Zero-Height SiSonic Microphone, Knowles Electronics) attached to the regions corresponding to the ear canals on both sides, ipsilateral and contralateral to TMS. Seven TMS intensities for both sham and real TMS conditions were tested, applying 25 pulses each at intensities from 20 to 80% of the MSO in 10% steps. By analyzing the absolute amplitude of the signal in the first 50 ms after the pulse (Fig. 1C), we observed an approximately linear relation between the sound amplitude generated by sham TMS and real TMS at different intensity (within the range of intensities between 20 and 50% MSO), i.e., the average sound pressure level from the sensors ipsilateral and contralateral to stimulation caused by real TMS could be matched by sham TMS when increasing sham TMS intensity by a factor of 1.6 (Fig. 1D).

To control for the somatosensory input, we aimed to reproduce the somatic input caused by real TMS by delivering ES using an electric stimulator and electrodes placed over the scalp. During a pilot experiment we explored several different stimulation intensities and electrode montages. This was necessary as the scalp sensations produced by TMS and ES were easily distinguishable: subjects reported real TMS as causing a blunt sensation in a broad area of the scalp and leading to a slight contraction of the temporal muscle, whereas the ES sensation was described as sharp and focal. We observed that shorter ES pulse widths were re-

ported as less sharp and more similar to TMS, leading us to set it to 50 μs, the lowest pulse width allowed by the stimulator. To generate a broad region covered by stimulation, and a cranial muscle twitch, we positioned 2 pairs of electrodes of 1 cm in diameter between the EEG electrodes over a broad area of the left fronto-temporal region: 2 electrodes of the same polarity at the positions corresponding to FFT9h and AFF5h, according to the international 10–5 system for EEG (Seeck et al., 2017), and 2 electrodes of opposite polarity at CPP3h and TPP7h (Fig. 1A).

Despite these efforts, we realized that individuals could still distinguish between the sham and real TMS sensory input. This could represent a significant limitation, as this discernibility might indicate different levels of sensory input between conditions, potentially eliciting PEPs with different characteristics. However, even an indistinguishable sham condition does not guarantee that the resulting PEPs from the two conditions are identical, which would have to be carefully tested to confirm the validity of the optimized sham condition.

Our strategy to overcome these problems was to use high-intensity ES applied to *both* sham and real TMS conditions. The rationale is that high enough ES intensities will saturate the somatosensory input. If successful, any further somatosensory input would not result in a detectable increase in the PEP amplitude, including the somatosensory input from real TMS.

By testing different ES intensities, set as multiples of the individual's sensory perception threshold (SPT), we anticipated PEP saturation to occur with intensities around 300% of the SPT, as suggested by previous reports (Torquati et al., 2002; Lin et al., 2003), and also by our own pilot measurements. The mean SPT of the final sample was 8.7 mA (SD ± 2.5 mA).

In summary, the sham TMS condition involved (Fig. 1E, lower part): (1) masking noise, (2) sham coil click (sham TMS coil on top of the real TMS coil, tilted by 90 °, intensity 1.6 × 90%RMT) and (3) concomitant application of ES (intensity as a function of the individual's SPT). The real TMS condition involved (Fig. 1E, upper part): (1) masking noise, (2) real coil stimulation (real TMS coil placed tangentially on the scalp, with peak induced electrical field targeting M1, intensity 90%RMT) and (3) concomitant application of ES (intensity as a function of the individual's SPT, identical to ES in the sham condition). Standard ES intensity was 300%SPT, but for a few subjects (n = 5) who could clearly distinguish between real and sham TMS conditions, the intensity was increased to 400%SPT.

2.4. Testing the optimized sham TMS condition

The first measurement was aimed to confirm the PEP saturation with increasing ES intensities. This involved the application of 5 stimulation blocks of 100 pulses each, applied with an interstimulus interval of 2 s (±1 s jitter; 1–3 s range), each containing the masking noise, auditory sham, and ES; but the ES intensity was different in each block: 0, 100, 200, 300 and 400%SPT. These blocks were delivered in pseudorandomized order balanced across subjects.

We also evaluated the perception of the real vs. sham TMS conditions with 2 different procedures. In the first procedure subjects received 4 blocks of 4 stimuli each, 2 blocks containing only the sham TMS condition and 2 blocks containing only the real TMS condition. The blocks were delivered in random order. Subjects were instructed to fill out a set of visual analog scales (VAS, values 0 to 10) after each block, referring to the perceived sensation during each block with regard to the following perception items: (1) intensity of auditory sensation; (2) intensity of scalp sensation; (3) area size of scalp sensation; (4) intensity of pain or discomfort. The second procedure consisted of a two-alternative forced choice (2AFC) test: Subjects were instructed as to the sensations caused by each condition, using stimuli probes as examples. Following that, subjects were given a panel with 2 buttons, one labeled "SHAM" and the other "REAL", and then 50 pulses were applied (25 of each condition in random order), and after each pulse subjects were forced to indicate whether they thought this was a sham or real condition by pressing the corresponding button.

The concluding TMS-EEG measurements consisted of the application of 320 pulses, 160 real TMS and 160 sham TMS, randomly interleaved and applied with an interstimulus interval of 3 s (±1 s jitter; 2–4 s range).

2.5. EEG data processing

Offline data analysis was performed using the Fieldtrip open source toolbox (Oostenveld et al., 2011). EEG data from TMS responses were segmented into epochs aligned to the TMS pulse (−1000 to 1500 ms) and baseline corrected (−1000 to −50 ms). Data containing artifacts from the TMS and ES pulses, and the associated muscle response were removed and cubic interpolated (−5 to +20 ms window around the TMS pulse). Trials were inspected visually, and epochs and channels with excessive noise were excluded, as were trials containing MEPs in the EMG of the right FDI or APB. The average percentage of trials excluded per subject was 17% (SD ± 12%; range: 4–26%), being on average 10.2% due to excessive noise (SD ± 6.5%; range: 4.6–23.8%) and 6.8% due to the presence of MEPs (SD ± 3.5%; range: 1.1–12.0%). The number of channels excluded due to excessive noise was on average 6 (SD ± 2.6; range: 1–12). Further artifacts were removed with a 2-step ICA procedure. The first step aimed at removing remnant high amplitude TMS and ES artifacts, and the second step removing artifacts related to muscle activity and eye blink (Rogasch et al., 2014). Excluded channels were spline-interpolated and the signal was then re-referenced to the average of all electrodes after the ICA procedure. The TEP signal was finally filtered with a 45 Hz low-pass filter. Furthermore, individual results were inspected for outliers, averaging the amplitude of the signal in 5 different time windows of interest (TOI: 25–40 ms, 40–60 ms, 60–90 ms, 90–130 ms and 130–250 ms), and indicating individual data deviating >3 standard deviations from the mean as outliers.

For the processing of TMS-induced oscillations, time–frequency representations (TFRs) of TMS-related changes in oscillatory power were calculated. First, the evoked TMS response (average signal time-locked to TMS stimulus) was subtracted from the signal, and the result was then decomposed into its TFRs (Premoli et al., 2017). TFR was then calculated using a Morlet wavelet decomposition on single trials, with frequency-dependent width (wavelet width of 2.6 cycles at 4 Hz, adding 0.2 cycle for each 1 Hz), followed by z-transforming the TFR of each trial with respect to the mean and standard deviation of the full trial, and baseline correction (−500 to −100 ms) (Premoli et al., 2017). By excluding the time-locked evoked response, we remove information regarding amplitude shifts of the evoked potential, which is an information already contained in the TEP analysis, thus focusing specifically in the changes in cortical oscillatory activity due to the stimuli.

Finally, the EEG signals from statistically significant results were projected into the source space. Individual cortical surfaces and dipole arrays were obtained from the individual's MRI, segmented and meshed using the Fieldtrip toolbox (Oostenveld et al., 2011), with a forward model for EEG using a customized pipeline, taking into account the positions of the EEG electrodes related to individual head anatomy (Stenroos and Sarvas, 2012; Stenroos and Nummenmaa, 2016). Source reconstruction was then obtained on the whole cortical surface using the L2-minimum-norm estimate (Hamalainen and Ilmoniemi, 1994). For the TEPs, the final result was obtained by z-transforming the signal of each trial with respect to the mean and standard deviation of the baseline (−500 to −100 ms). For induced oscillations, the EEG signal was first projected to the source space, followed by the TFR calculation, as described above. Finally, for the purpose of plotting the final result, data attributed to each individual dipole was pooled and warped into a common MNI space for a group average across all subjects.

2.6. Statistical analysis

All statistical analyses were performed on the MATLAB platform (R2018b, The Mathworks, USA). Data from the visual analog scales in

the sham and real TMS conditions were analyzed using paired comparisons, with significance threshold of $p < 0.0125$ to adjust for multiple comparisons. Given the marked skewness of some distributions, we used two-sided Wilcoxon rank sum tests for these analyses. Responses from the 2AFC test were pooled individually in order to yield each subjects accuracy (total correct answers divided by total number of trials). The individual accuracy was subtracted by the expected accuracy for random answers (0.5). The absolute value of this transformation corresponds to the distance of the observed accuracy and the expected accuracy for random answers. In order to identify the likelihood that the observed distance deviated significantly from random answers (i.e., in this case the subject was able to distinguish between sham and real TMS conditions), the distance was compared with the distribution of the medians derived from 100,000 simulations of 23 subjects responding to the test randomly.

For the PEPs elicited by different ES intensities, the signal was first analyzed by its global mean field power (GMFP) within time windows of interest (TOI) 60–90 ms, 90–130 ms and 130–250 ms after the ES pulse, based on previous reports on TMS-EEG and PEP signals (Lioumis et al., 2009; Rocchi et al., 2021). GMFP in the 5 stimulation conditions (ES intensities, 0–400%SPT, in 100% steps) were compared using one-way ANOVA. The EEG signals from the 300%SPT and 400%SPT conditions were compared by cluster-based dependent-samples t-tests from the Fieldtrip open source toolbox, using as input the averaged signal across trials for each subject, and setting the statistical threshold to $p < 0.05$ (Oostenveld et al., 2011).

Analysis of the TEPs from the real vs. sham TMS conditions was performed with identical cluster-based t-statistics. Analysis of the induced oscillations followed the same procedure, but was divided into different frequency bands of interest: theta (4–7 Hz), alpha (8–12 Hz), low beta (13–20 Hz), high beta (21–29 Hz), and gamma (30–40 Hz). Due to the increased number of tests, the threshold of statistical significance was adjusted to $p < 0.01$.

3. Results

3.1. Testing the optimized sham TMS condition – peripherally evoked potentials

We first tested the optimized sham TMS by delivering ES of increasing intensities, while concomitantly applying masking noise and auditory sham stimulation (Fig. 1E). We observed that despite the masking noise, auditory sham stimulation alone (ES set to 0%SPT, Audit.only) evoked an EEG response in central midline electrodes, starting at around 130 ms and peaking at 200 ms, albeit of small amplitude (Fig. 2A–C).

The GMFP amplitude increased with increasing ES intensity and reached a plateau with intensities ≥ 300%SPT (Fig. 2A). We tested this by comparing the GMFP across conditions in 3 different TOIs (Fig. 2D). 300%SPT and 400%SPT conditions were not different for the TOIs 90–130 ms and 130–250 ms (ANOVA $p < 0.001$; *post hoc* Audit.only = 100%SPT < 300%SPT = 400%SPT). For the TOI 60–90 ms, although there was no statistically significant difference between 300%SPT and 400%SPT, the results were not equivalent (ANOVA $p = 0.002$; *post hoc* Audit.only = 100%SPT = 200%SPT < 400%SPT). We further tested possible differences between the PEPs from the 300%SPT and 400%SPT conditions by comparing the respective EEG responses using a cluster-based *t*-test. The test revealed 2 significant clusters between 70 and 100 ms, with a higher signal amplitude in the 400%SPT condition (Fig. 2E–F). By subtracting the results from the source reconstruction of both signals in that time window, we observed that the difference was most pronounced over bilateral sensorimotor cortices (Fig. 2G). No significant differences were found beyond 100 ms.

3.2. Testing the optimized sham TMS condition – sensory perception

We compared the sensory perception from the sham and real TMS conditions using the results from the VAS. The reported sensory perceptions were not significantly different between conditions for any of the tested sensorial qualities (Fig. 3A, two-sided Wilcoxon rank sum tests: auditory intensity, $p = 0.596$; scalp intensity, $p = 0.938$; scalp area, $p = 0.484$; pain/discomfort, $p = 0.999$).

The results from the 2AFC test are shown in Fig. 3B, displayed as the distance of the individuals' accuracy to 50% (i.e., distance to expected accuracy of random responses). In our sample, the subjects' median "distance from 50% accuracy" was 0.1. By running simulations of 23 subjects answering randomly to this test, we obtained that the mean of the simulated median "distance from 50% accuracy" is 0.03 (SD ± 0.005). This places the observed median distance outside 5 SD of the simulated distribution, indicating a probability $p < 0.0001$ that our subjects as a whole sample responded randomly to the 2AFC test. This can be exemplified by the presence of 3 clear outliers (Fig. 3B-C), who were most definitely capable of making the distinction between conditions ($p<0.00001$ that any individual would attain "distance from 50% accuracy" > 0.4 by answering randomly). Note that one outlier actually had an accuracy close to zero (Fig. 3C). It is most likely that this individual could indeed make the distinction, but mistook sham TMS for real TMS, and vice versa. Since the issue is discernibility between conditions, this reinforces using the "distance from 50% accuracy" in this study, rather than accuracy *per se*.

Even after exclusion of the 3 outliers, the median "distance from 50% accuracy" was still > 5 SD away from the expected median (now simulated with $n = 20$ subjects), suggesting that at least some individuals were still somewhat capable of making a distinction between the sham and real TMS conditions. Based on the 2AFC test results we divided the sample into two groups: subjects with a small distance from 50% accuracy were considered as being "unaware" of the condition, and those with larger distance as being "aware". This procedure was performed by selecting a threshold, estimated by progressively excluding subjects with the largest distance from 50% accuracy from the statistical analysis, and correspondingly readjusting the simulation's sample size, until we obtained a median < 2 SD away from the expected median for random answers. This was reached with a threshold distance from 50% accuracy of 0.12. A total of 13 subjects (56%) were classified as "unaware" and 10 subjects (44%) as "aware".

We investigated what could have caused individuals to be able to distinguish between the sham and real TMS conditions. We first considered that the use of high TMS intensities (subjects with high RMT) or lower ES intensities (subjects with low SPT) could have been prone to distinguishable sensory inputs. However, there was no evidence for differences in TMS or ES intensities between the "aware" and "unaware" subjects (Fig. 3D, two-sided Wilcoxon rank sum test: TMS $p = 0.900$; ES $p = 0.729$). Moreover, subjects who were particularly accurate in identifying the conditions ("highly aware", corresponding to the 3 outliers. Fig. 3B, C.) did not appear to have skewed the distributions in any direction. We also investigated whether the perception of the different items of sensory input as quantified on the VAS could have explained the distinction. Likewise, there was no significant difference in the reported sensory perception regarding auditory intensity ($p = 0.642$), somatic scalp intensity ($p = 0.696$) or pain/discomfort ($p = 0.394$). Only a non-significant trend was observed towards reporting larger scalp area perception in the real TMS compared to sham condition in subjects who were "aware" ($p = 0.040$, significance threshold $p < 0.0125$; Fig. 3E). Again, the subjects who were "highly aware" of the difference did not appear to have affected these distributions.

3.3. Comparing sham and real – TMS evoked potentials

On inspection of the results of all individual subjects, we identified one subject as an outlier (amplitude of the signal in TOI 25–40 ms > 3 SD, TOI 130–250 ms > 3 SD, and TOI 90–130 ms > 4 SD, see Supplementary Results). This subject was therefore excluded from the ensuing analyses. No other subject presented deviations > 3 SD in any TOI. We then compared the evoked EEG responses in the sham and real

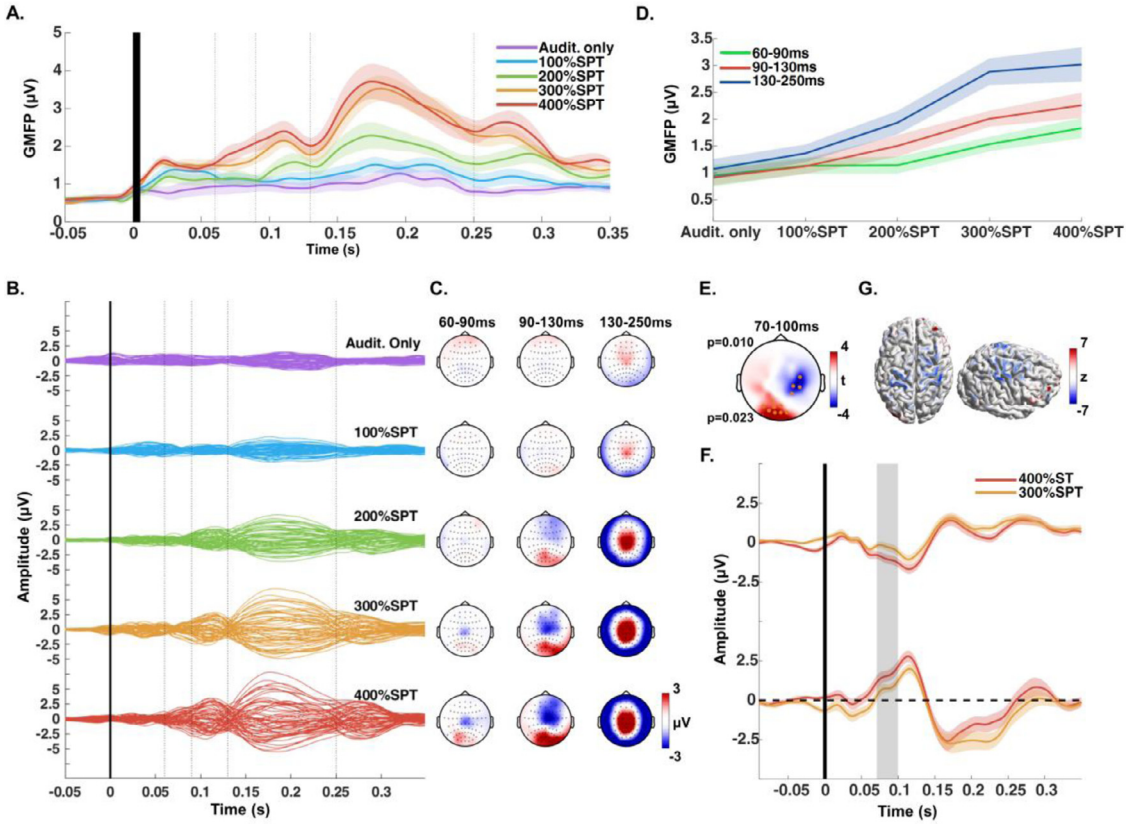

Fig. 2. **A.** Global mean field power (GMFP), averaged across all subjects, from the EEG responses to the sham condition with different electric stimulation intensities, set as multiples of the individual's sensory perception threshold (SPT). Dotted lines indicate the boundaries of the time windows of interest (TOIs). Audit.only indicates that no electric stimulation was applied. Please note that the filtering shifted the onset of EEG responses leftward. **B.** Butterfly plots of the averaged EEG response across all subjects, divided by increasing intensity of the electric stimulation (average reference, each line corresponding to one EEG channel) **C**. Scalp distribution of the signal observed in B, divided in 3 TOIs. **D**. Increase of the averaged GMFP within each TOI with increasing intensity of the electric stimulation. **E.** Results of the cluster-based *t*-test comparing the conditions applying electric stimulation intensity at 300% SPT vs. 400%SPT, showing two significant clusters (electrodes within the clusters marked by orange dots, respective *p*-values on the left) between 70 and 100 ms after the stimulus. **F.** EEG signal over time, averaged across the electrodes from the negative cluster (top plot) and positive cluster (bottom plot), from the 300%SPT and 400%SPT conditions. The shaded gray areas correspond to the time windows where the significant clusters were found **G.** Display of the difference of the EEG signal (400%SPT minus 300%SPT) within 70–100 ms, projected to the source and normalized with respect to the baseline signal (*z*-value) (For interpretation of the references to color in this figure legend, the reader is referred to the web version of this article).

TMS conditions (Fig. 4A, B). This comparison revealed significant differences, shown as a series of clusters of channels in TOIs 25–50 ms, 40–50 ms, 70–90 ms, 100–150 ms and 480–520 ms (Fig. 4C-D). More specifically, the real TMS condition caused an early positive deflection around 30 ms (P30) after stimulation in central electrodes close to the site of real TMS over left M1. This was followed by a dipole, consisting of a negative deflection around 45 ms in frontal electrodes in the midline and non-stimulated hemisphere (N45) and a positive deflection in parietal electrodes of the stimulated hemisphere (P45). This turned into a dipole of reverse polarity at around 70 ms (P70 over frontal electrodes in the non-stimulated hemisphere, N70 over parieto-occipital electrodes in the stimulated hemisphere). Moreover, while both real and sham conditions presented the deflection typically attributed to PEP, involving a frontocentral negative deflection at 100 ms (N100), the difference (real – sham TMS) suggests that real TMS caused a positive deflection peaking at around 125 ms, centered at the stimulated region of left M1 (P120). Finally, the real TMS condition evoked a long-latency positivity that peaked at central electrodes around 500 ms after the pulse (P500). Similar results were also found when only investigating subjects that were "unaware" of the difference between sham and real TMS conditions (Supplementary Results), providing evidence that the capability of distinguishing between the sham vs. real TMS conditions played no role in the TEP findings. The projection of the EEG signals to the source, followed by the subtraction of the sham from the real TMS condition suggested that P30 involves a broad response centered on the sensorimotor cortex ipsilateral to the stimulation, the N45 / P45 responses in bilateral prefrontal cortex / centered on the ipsilateral somatosensory cortex, the P70 / N70 responses in the bilateral prefrontal cortex / ipsilateral parietal cortex, and the P120 and P500 responses in the stimulated sensorimotor cortex (Fig. 4E).

3.4. Comparing sham and real – transient TMS-induced increase in beta band power

Both the sham and real TMS conditions led to considerable changes in the ongoing oscillations, with increased power in all of the investigated frequency bands after stimulation (Fig. 5A). Statistical comparison of the TFRs revealed significant differences (real TMS > sham TMS) in the low (13–20 Hz) and high beta bands (21–29 Hz) in time windows between 50 and 140–160 ms (Fig. 5B, C). These differences were expressed in the stimulated sensorimotor cortex and frontal cortex mainly ipsilateral to stimulation (Fig. 5B–D).

Spectral power changes were not different between the TFRs of sham and real TMS conditions in any other of the tested frequency bands (Fig. 5A and C).

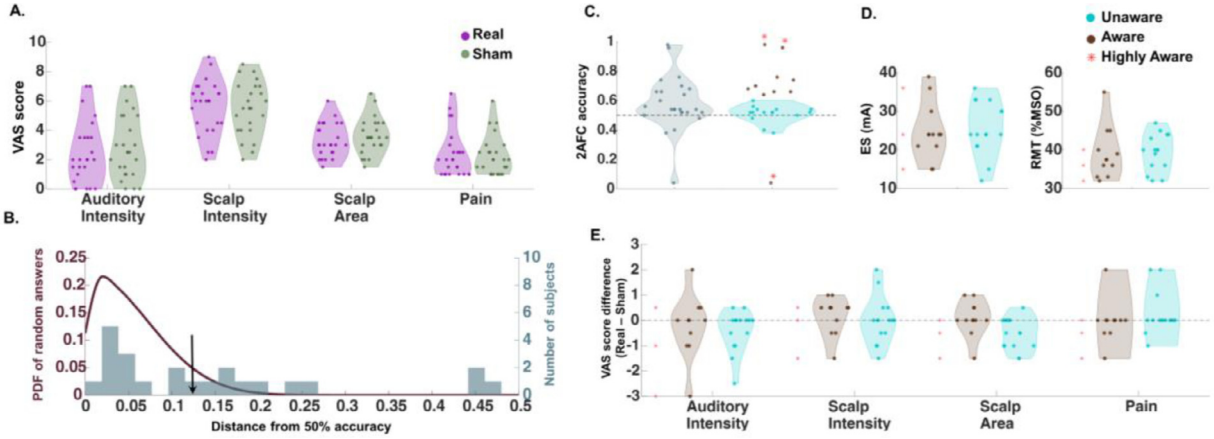

Fig. 3. **A.** Results from the visual analog scale for perceived stimuli sensation from the sham and real TMS conditions, each dot corresponds to an individual subject. **B.** Histogram of the 2AFC test's response, shown by the individuals' "distance from 50% accuracy" (grey), plotted with the expected value of the "distance from 50% accuracy" in case of random answers, shown as a probability density function (PDF) (brown). The arrow points to the threshold that divides subjects classified as being "unaware" of the distinction between the sham and real TMS condition (to the left from the arrow) and those who were "aware" (to the right). **C.** Left plot showing the overall accuracy of the subjects to the 2AFC test, and the right plot showing the same data, but separating subjects who were "unaware" (cyan) and subjects who were "aware" (brown) as to the distinction between the sham and real TMS conditions. The dots correspond to individual subjects and red asterisks indicate those subjects who were "highly aware" of the distinction. **D.** Comparison of "aware" and "unaware" subjects with respect of the ES and the TMS intensities used in the experiment, red asterisks indicating the values from the subjects who were "highly aware" of the distinction. **E.** Comparison of the "aware" and "unaware" subjects with respect of the difference of reported sensory perceptions on the visual analog scale (VAS) from each condition (real minus sham) (For interpretation of the references to color in this figure legend, the reader is referred to the web version of this article).

4. Discussion

4.1. Design and test of the optimized sham

Designing an ideal sham condition for TMS-EEG experiments is particularly challenging as, despite best efforts, sham conditions often fail to match the multisensory input from the real TMS condition (Conde et al., 2019). Given that this constitutes a major caveat of the method, it is unfortunate that most previous studies have not properly reported the subjects' perceived sensory input from real and sham conditions. In some cases only the auditory input was assessed (Rocchi et al., 2021), or only accuracy of distinction between conditions was tested (Mennemeier et al., 2009; Gordon et al., 2018), or the perceived stimulus intensity scale was solely used to set the sham intensity (Opitz et al., 2014).

The notion that most of the PEPs in TMS-EEG are attributed to auditory inputs (Paus et al., 2001; Ilmoniemi and Kicic, 2010) has probably drawn exceeding attention to this issue, leading subsequent studies to neglect the impact of somatosensory inputs. For instance, Du et al. investigated the effects of TMS to several cortical areas, but did not include a somatosensory control (Du et al., 2017). The EEG signal in the sham condition was of markedly low amplitude, and the authors attributed the frontal N100, observed at all stimulation sites, to a generic marker of direct brain activation by TMS (Du et al., 2017). This view can no longer be maintained, given the results observed here and by others (Conde et al., 2019; Ahn and Frohlich, 2021) demonstrating that the N100 is predominantly a peripherally evoked potential. Harquel et al. (2016), although correctly identifying the P200 present in all the experimental conditions as an auditory evoked potential, did not consider a possible contribution by somatosensory input .

Other studies, although including somatosensory sham control, have likely failed to employ a condition that properly matched the sensory input from real TMS. A recent report used a combined auditory and somatosensory sham approach aiming to disentangle the PEPs from the TMS-EEG signal (Rocchi et al., 2021). The study applied proper noise masking that suppressed the auditory evoked potential; however, it employed a somatosensory sham condition with electric stimulation of low intensity (on average, 6 mA), which most likely did not match the TMS somatic input. This can also be inferred from the low amplitude of the EEG response evoked by this condition, which led to a N100 potential in frontocentral regions following real TMS, most likely representing a residual PEP that was not adequately controlled for by the sham condition (Rocchi et al., 2021). One example of a more adequate control for somatosensory inputs is reported by Raffin et al. (2020), who analyzed the EEG responses to increasing TMS intensities, while also attempting to match the sensory input by increasing ES intensities (Raffin et al., 2020).

In order to overcome the limitations from these previous studies, we designed our optimized sham condition by considering these sources of sensory input from the TMS activation, auditory and somatosensory, and tested our design with a psychophysical comparison of the sham and real TMS perception. We observed that the GMFP from the auditory sham condition (Fig. 2A) was of lower amplitude than reported from sham stimuli without masking noise (Gosseries et al., 2015; Rocchi et al., 2021), corroborating a considerable suppression of the auditory evoked potential by masking. Still, a small-amplitude potential remained in a period of 130–250 ms after stimulation (Fig. 2A–C). This justifies the use of an auditory sham stimulation with equivalent sound pressure level at the ear canal compared to the real TMS condition (Fig. 1C, D), thus helping to create indistinguishable conditions. To control for the somatosensory evoked potential we applied electric stimuli to the scalp area of the TMS target, aiming to generate a highly similar somatic input to the real TMS and keeping the subject unaware as to the nature of each stimulus (Rossi et al., 2007; Mennemeier et al., 2009), a feature that cannot be claimed by other sham modalities such as shoulder stimulation (Herring et al., 2015; Biabani et al., 2019). However, only when adding the ES to both real and sham conditions subjects reported a thoroughly comparable sensory perception from these conditions.

The use of this optimized sham procedure might also be of particular advantage as a placebo condition for clinical trials using TMS. Clinical trials using non-invasive brain stimulation also face significant validity issues due to the challenge of applying a sham that consistently simulates the real TMS, which is especially problematic given the substantial placebo effect attributed to TMS (Razza et al., 2018; Burke et al., 2019). Although originally only auditory stimulation was included as sham, to properly simulate the real TMS, further sham procedures also integrated

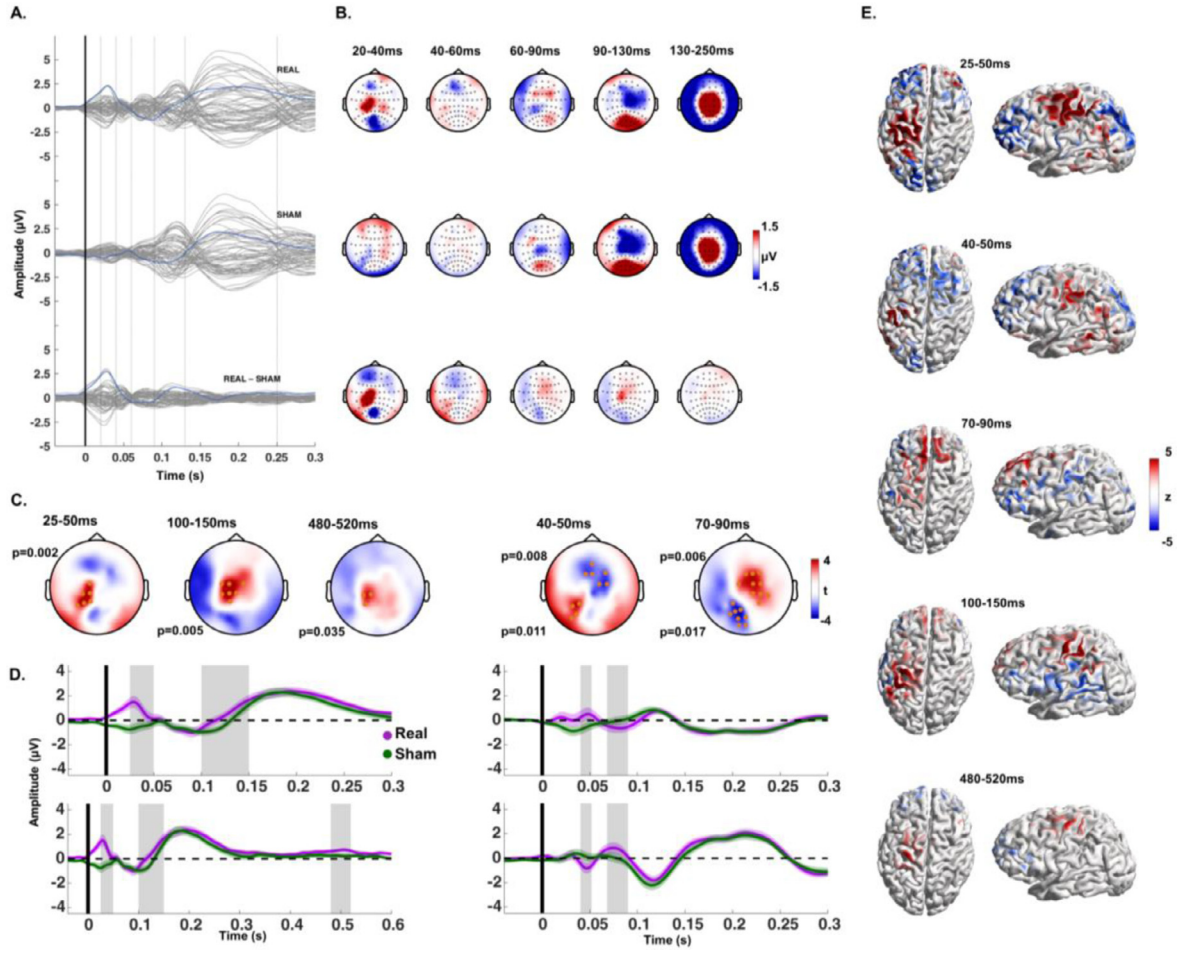

Fig. 4. **A.** Butterfly plots of the averaged EEG response across all subjects, divided by real TMS condition, sham TMS condition and the subtraction of the sham from the real condition (average reference, each line corresponding to an EEG channel, blue line corresponding to the C3 channel, i.e., close to the site of real TMS) **B.** Scalp distribution of the signal observed in A, divided in 5 time windows of interest. **C.** Results of the cluster-based *t*-test comparing the sham and real TMS conditions showing two significant clusters, displayed as resulting t-values of each electrode (electrodes in the clusters marked by orange dots, respective p-values on the left). **D.** Signal over time of EEG responses from the real TMS (purple) and sham TMS (green), triggered at time=0 (black line). Plots in the left column show the signal from the electrodes that composed the clusters indicated in C: 25–50 ms, 100–150 ms and 480–520 ms (note that only the bottom plot shows the 480–520 ms cluster). Plots in the right column show the signal from the electrodes that composed the clusters indicated in C: 40–50 ms and 70–90 ms (top plot corresponds to the fronto-central cluster and bottom plot to the left-hemispheric sensorimotor cluster). Shaded grey areas correspond to the time windows of the clusters (indicated in C). **E.** Difference of the source projection, displayed as *z*-scores, of the real minus sham condition EEG signals, in the time windows where the significant clusters were found (For interpretation of the references to color in this figure legend, the reader is referred to the web version of this article).

somatosensory stimulation by the means of scalp electrical stimulation (Rossi et al., 2007; Mennemeier et al., 2009). Our optimized sham goes one step further by applying electrical stimulation to both real and sham, assuring equivalent subjective perception in multiple sensory modalities and an overall indistinguishability between conditions. The method may prove capable of fully homogenizing the placebo effects of real and sham TMS in a clinical trial, thus revealing the true therapeutic effect of non-invasive brain stimulation. This, however, will require further testing.

4.2. Separating TEPs from PEPs

In TMS-EEG experiments, the sham condition must also reliably control for the peripherally evoked responses in the EEG caused by real TMS. Several procedures have been proposed to clear TMS-EEG data from PEPs, including ICA, and linear regression or cosine similarity-based analysis (Biabani et al., 2019; Freedberg et al., 2020; Raffin et al., 2020). However, these methods do not exempt the need of a sham condition, as it is necessary to inform the models what constitutes a PEP, so it can then be removed from the real TMS response. Moreover, some of these methods rely on further assumptions; for instance, ICA assumes temporal independence of the underlying sources, an assumption that is very likely violated given that both TEPs and PEPs are time-locked to the stimulus (Biabani et al., 2019).

An even more far-reaching assumption is that the TEPs and PEPs are independent phenomena and do not exert any influence on each other, meaning that their corresponding EEG signals are simply linearly superimposed. This assumption is the basis of most proposed methods so far to remove PEPs from TMS-EEG responses (Biabani et al., 2019), and also necessary for statistical comparisons between real and sham TMS conditions, as they have been widely performed in previous studies (Herring et al., 2015; ter Braack et al., 2015; Du et al., 2017; Gordon et al., 2018; Raffin et al., 2020; Rocchi et al., 2021). However, the assumption that TEPs and PEPs do not interact is unlikely, given the converging evidence for modulatory effects of sensory input on motor cortex excitability (Novembre et al., 2019) (for review (Kenemans, 2015; Wessel and Aron, 2017)). As a consequence, changes in cortical excitability induced by the multisensory TMS-induced inputs, which include vibration, tactile sensation, direct activation of trigeminal afferents and contraction of cranial muscles, likely cause changes to the

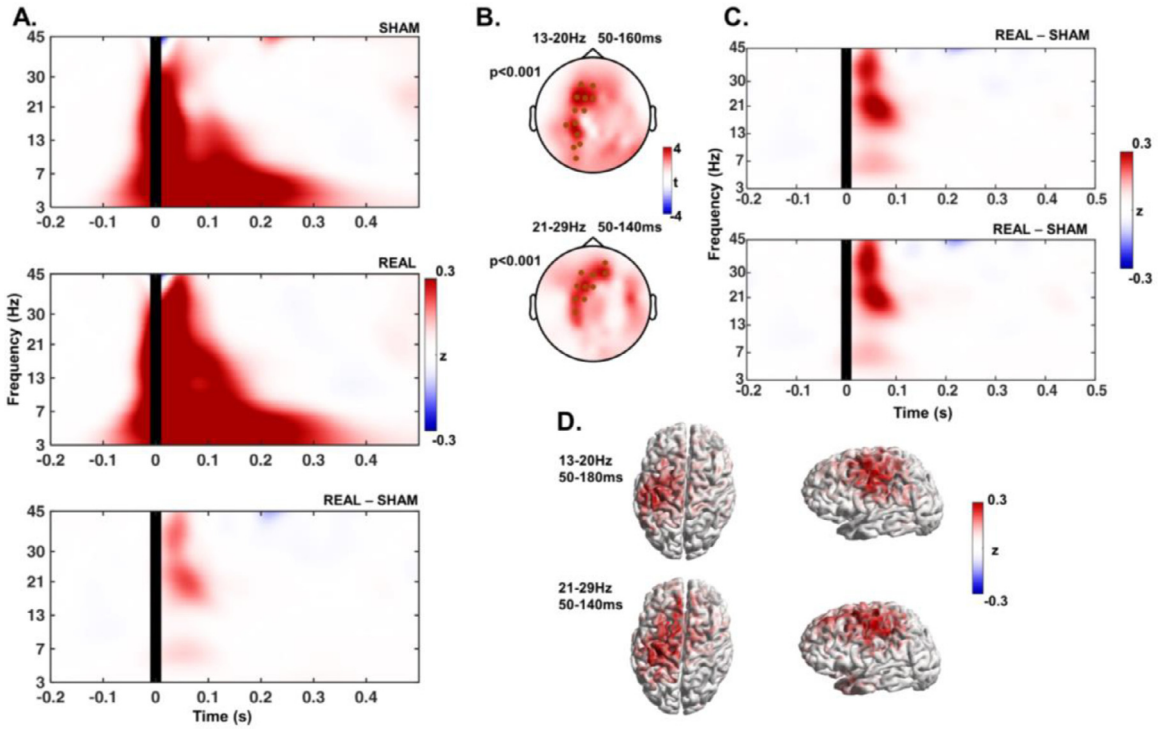

Fig. 5. **A.** Time-frequency response (TFR) plots show the change in spectral power with respect to baseline, averaged across all subjects and electrodes, from the sham and real TMS condition, and the subtraction of the sham TFR from the real. **B**. Results of the cluster-based t-tests comparing the real and sham conditions showing two significant clusters (marked as black dots, respective *p*-values on the left) in the low beta band (13–20 Hz) around 50–160 ms after the stimuli, and a single cluster in the high beta band (21–29 Hz) around 50–140 ms after the stimuli, displayed as *t*-values of each electrode. **C.** TFR plots show the response to the real TMS condition after subtraction of the sham condition, with the TFR shown in each plot corresponding to the average signal of the electrodes that composed the clusters indicated in B (top-plot corresponds to the 13–20 Hz cluster and bottom-plot to the 21–29 Hz cluster). **D**. Difference of the source reconstruction of the oscillatory response to real TMS minus sham condition, displayed as *z*-scores, in the frequency bands and time windows where the significant clusters were found.

"true" TEP that would be obtained by direct cortical activation in isolation. Even though the issue has not been explored in TMS-EEG studies, this interaction imposes a significant limitation to the aforementioned methods to remove PEPs from TMS-EEG responses.

Despite these limitations, we chose to follow previous studies in the assumption of linear superposition, which is a prerequisite for the subtraction of the sham response from the real TMS response. It follows that the resulting signals should not be understood as corresponding to "true" TEPs, due to the potential modulatory effect of the sensory input. Nevertheless, by designing a method that generates closely comparable sensory inputs and evoked potentials in sham and real TMS conditions, we could consistently match PEP contributions in the real and sham condition. We accomplished this by applying supramaximal ES in sham and real TMS conditions, thereby saturating the EEG responses to somatosensory input. Logarithmic input-output curves have been demonstrated for PEPs, i.e., linear increases of stimulus intensity result in progressively smaller increases in PEP amplitude, approaching asymptotically a plateau (Torquati et al., 2002; Lin et al., 2003). We demonstrated saturation of PEP amplitude at ES intensities ≥ 300%SPT (Fig. 2). An early-latency PEP component at around 80 ms, however, did not reach a plateau (Fig. 2D–G). Nevertheless, the comparison of the EEG signals in the real minus sham TMS conditions revealed a potential of opposite polarity in this time window of interest (Fig. 4C), indicating that an incomplete saturation of this early somatosensory potential, if anything, had resulted in underestimation of the amplitude of the underlying TEP.

The results from using the present method to remove PEPs from early (i.e., within the first 90 ms) EEG responses to TMS of motor cortex are mostly in agreement with previous reports (for review, (Komssi and Kahkonen, 2006; Hill et al., 2016; Hallett et al., 2017)). However, a close inspection shows that only the P30 and the N45/P45 have been clearly described, while a dipolar P70/N70 with the P70 expressed in bilateral prefrontal cortex and the N70 in parietal cortex ipsilateral to TMS was not described in uncontrolled or incompletely sham-controlled studies (Komssi et al., 2004; Bonato et al., 2006; Premoli et al., 2014; Cash et al., 2017; Gordon et al., 2018; Darmani and Ziemann, 2019; Ahn and Frohlich, 2021; Belardinelli et al., 2021), with the exception of one study that however failed to demonstrate the preceding dipolar N45/P45 response (Premoli et al., 2014). A recent study has described a negative deflection at around 45 ms and a positive deflection at 60 ms, respectively N45 and P60, which were located in the ipsilateral somatosensory cortex, whereas the P30 was localized in the stimulated motor cortex, in line with our present findings (Ahn and Frohlich, 2021).

The confirmation of early TEPs (below 100 ms after the TMS pulse) was expected, as this time windows is mostly free of PEPs (Conde et al., 2019; Ahn and Frohlich, 2021). Beyond 100 ms the superposition of the PEPs hinders the analysis of TEPs, and sham control procedures that do not fully reproduce the sensory input from the real TMS may lead to components of PEPs erroneously interpreted as TEPs. Using the present optimized sham procedure, we observed a close match of the EEG signals from the sham and real TMS conditions beyond 100 ms, despite the real TMS condition contained objectively more sensory input (TMS + ES). This supports that we attained PEP saturation and that the resulting PEPs from both conditions was equivalent, representing a thorough control of multisensory input in the real TMS condition by the sham condition.

Nevertheless, we were able to identify significant differences in this time window that can most likely be attributed to direct cortical activation by TMS, namely positive deflections around 120–130 ms and 480–520 ms after the TMS pulse (Fig. 4). These differ from PEPs as their peaks are shifted from the expected PEPs, and they are located

specifically in the stimulated cortical region, the left M1, further suggesting that they correspond to direct cortical activation responses. The existence of a response specific to TMS activation around 120 ms has also been suggested by previous studies, despite these being partially or mostly attributed to sensory inputs in the form of PEPs (Nikulin et al., 2003; Komssi et al., 2004; Lioumis et al., 2009; Herring et al., 2015). In line with this, several interventions that aimed at modulating cortical excitability identified changes in the response signal within this time window (Premoli et al., 2014; Cash et al., 2017; Chung et al., 2019), but retrospective interpretation needs to acknowledge the possibility that these changes are combined effects of intervention on TEPs and PEPs. Finally, we found a significant positivity in the stimulated area around 500 ms after the stimulus, specific to the real TMS condition, which might have gone undetected in previous reports by being in a time window beyond of what usually is investigated in TMS-EEG studies, and might deserve further investigation of its relevance and physiological implication.

4.3. Extracting sensory induced oscillations from TMS induced oscillations

The results presented here corroborate the notion that also cortical oscillatory activity can be modulated by indirect sensory input. Both real and sham TMS induced considerable changes in the oscillatory activity, observed by a power increase in all of the analyzed frequency bands immediately after stimulation (Fig. 5). After subtracting the EEG signals of the sham from the real TMS condition we observed that the only remaining oscillatory change is an increased beta power within the first 200 ms, mostly located in the stimulated sensorimotor cortex. The induced increase in beta oscillations (13–29 Hz) most likely reflects direct TMS responses typical of motor cortex, whereas lower frequency responses that have been eliminated by subtraction of the sham from the real TMS condition likely correspond to activity induced by sensory input (Rosanova et al., 2009; Fecchio et al., 2017; Biabani et al., 2021).

Our previous report on TMS-induced oscillations found differences between sham and real TMS conditions that are replicated in the present report, concerning the early increase in beta power while, retrospectively, later decreases in alpha and beta power likely have to be attributed to induced oscillations resulting from non-controlled sensory inputs (Gordon et al., 2018). The same problem occurred in other studies that did not apply a realistic sham control (Fuggetta et al., 2005; Fecchio et al., 2017). These examples underscore the importance of masking and matching sensory inputs, as it has been largely achieved in this study.

4.4. Limitations

Despite achieving a method that could remove PEP components in a TMS-EEG experiment, caution should be applied with respect to generalization of the reported findings. It is well recognized that TMS applied to different cortical regions and at different stimulus intensities leads to different cortical responses, mostly due to different neuronal populations being activated (Komssi et al., 2004; Rosanova et al., 2009). It follows that the present methodological procedures and findings cannot be simply transposed to TMS of other cortical areas or intensities, given that the present measurements were limited to subthreshold stimulation of motor cortex. Changing the cortical target may require adapting the sham condition. For example, use of high-intensity TMS, such as required for stimulating the cerebellum (Fernandez et al., 2021) may generate a sensory input of greater order of magnitude compared to the sham procedure described here, and thus a higher-intensity sham sensory control would be necessary for saturation of PEPs. Also, the sound pressure level equivalence function (Fig. 1D) will require recalibration if the real and sham TMS coils are moved to a different target. Finally, as mentioned before, the results cannot be generalized to TMS-EEG responses elicited by suprathreshold intensities, which have different characteristics, including higher amplitudes. Nevertheless, suprathreshold TMS pulses to M1 lead by definition to MEPs, which are responsible for an additional re-afferent somatosensory evoked response (Komssi et al., 2004; Fecchio et al., 2017; Premoli et al., 2017; Biabani et al., 2021). This response would further add to confounding signals to TEPs and induced oscillations.

Further technical aspects of the sham procedure deserve critical review. Firstly, whereas the real TMS coil was placed in contact with the scalp, the sham coil was placed atop the real coil (Fig. 1B, E). This led to different degrees of auditory input via bone conduction between sham and real TMS. The use of a spacer underneath the real TMS coil (Ruddy et al., 2018) would have allowed avoidance of vibratory input from both conditions. However, this would have required higher TMS intensities for effective cortical stimulation, and higher air conduction auditory input in the auditory sham control, with a possible compromising effect on the linear relation of real/sham sound pressure level (Fig. 1C, D). The close match of the EEG signals in the sham and real TMS conditions between 100 and 200 ms indicates that these slight differences in the sensory input did not result in a detectable PEP difference. Another issue concerns the electrical stimulation to control for somatosensory input. ES caused a sizable decaying artifact after the stimulus, due to the proximity of ES and EEG electrodes, requiring discarding the EEG signal in the first 25 ms after the stimulus. This may have resulted in omission of short-latency TEPs (Ilmoniemi et al., 1997; Ferreri et al., 2011).

Finally, the delivery of considerable multisensory input in both real and sham conditions might have altered the genuine TEP signature. Although TMS-EEG measurements in general might be subject to this effect due to the ubiquity of sensory stimuli from TMS, by applying peripheral stimulation at supramaximal intensity likely has increased the risk of changing the spatiotemporal patterns of the transcranially evoked EEG signature, as increased sensory inputs lead to more pronounced motor cortex modulation (Novembre et al., 2019). As a result, although the differences we observed successfully removed PEP components from the EEG response, there is no guarantee that the remaining TEP responses have not been warped by sensory inputs, and thus may not represent “true” TEPs.

These observations suggest that, despite its success in the objectives proposed in this study, the method of optimized sham need to be further developed. Matching the PEP corresponding to the motor re-afferent feedback will allow investigation of suprathreshold TMS intensities in studies of motor cortex. Future studies may also calibrate the optimized sham procedure, possibly lowering the amount of sensory stimulus needed for a consistent TEP and PEP pairing, thus minimizing the potential confounding effects of sensory input on the TEP response.

5. Conclusions

We present here an optimized sham for TMS-EEG experiments of the primary motor cortex hand area that matched the multisensory input from the real TMS condition, by delivering masking noise in addition to an auditory sham, combined with supramaximal somatosensory stimuli in both sham and real TMS conditions to saturate the PEPs. This method enables the identification of EEG responses caused by the direct cortical activation with TMS, while removing responses attributed to the procedure’s multisensory input.

Declaration of Competing Interest

P.C.G. and C.Z. report funding through the EXIST translational research program from the German Federal Ministry for Economic Affairs and Energy. H.S. received honoraria as speaker from Sanofi Genzyme, Denmark and Novartis, Denmark, as consultant from Sanofi Genzyme, Denmark, Lophora, Denmark, and Lundbeck AS, Denmark, and as editor-in-chief (Neuroimage Clinical) and senior editor (NeuroImage) from Elsevier Publishers, Amsterdam, The Netherlands. He has received royalties as book editor from Springer Publishers, Stuttgart, Germany and from Gyldendal Publishers, Copenhagen, Denmark. U.Z. received

grants from the German Ministry of Education and Research (BMBF), European Research Council (ERC), German Research Foundation (DFG), Janssen Pharmaceuticals NV and Takeda Pharmaceutical Company Ltd., and consulting fees from Bayer Vital GmbH, Pfizer GmbH and CorTec GmbH, all not related to this work. The other authors declare no further competing financial interests.

Credit authorship contribution statement

Pedro C. Gordon: Conceptualization, Visualization, Investigation, Formal analysis, Data curation, Writing – review & editing. **D. Blair Jovellar:** Investigation, Writing – review & editing. **YuFei Song:** Investigation, Writing – review & editing. **Christoph Zrenner:** Investigation, Writing – review & editing. **Paolo Belardinelli:** Formal analysis, Visualization, Conceptualization, Writing – review & editing. **Hartwig Roman Siebner:** Conceptualization, Visualization, Writing – review & editing. **Ulf Ziemann:** Conceptualization, Visualization, Writing – review & editing.

Data and code availability statement

MATLAB scripts—including the EEG pre-processing pipeline and statistics—are available at https://github.com/pcgordon/optimized_supraliminal_sham. These codes were designed for using the open source toolbox Fieldtrip, version 20210212 (https://www.fieldtriptoolbox.org/).

Data can be made available upon request.

Ethics statement

This study was conducted in accordance with the Declaration of Helsinki and following approval from the local ethics committee of the medical faculty of the University of Tübingen (registration number 456/2019BO2). The inclusion of subjects and data gathering started only after their signing the written informed consent approved by the local ethics committee.

Acknowledgments

C.Z. acknowledges support from the Clinician Scientist Program at the Faculty of Medicine at the University of Tübingen [grant number 391–0-0]. The project has received funding from the European Research Council (ERC Synergy) under the European Union's Horizon 2020 research and innovation program (ConnectToBrain) [grant number 810377], and from an EXIST Transfer of Research grant by the German Federal Ministry for Economic Affairs and Energy [grant number 03EFJBW169]. H.S. holds a 5-year professorship in precision medicine at the Faculty of Health Sciences and Medicine, University of Copenhagen which is sponsored by the [grant number R186–2015–2138].

Supplementary materials

Supplementary material associated with this article can be found, in the online version, at doi:10.1016/j.neuroimage.2021.118708.

References

Ahn, S., Frohlich, F., 2021. Pinging the brain with transcranial magnetic stimulation reveals cortical reactivity in time and space. Brain Stimul. 14 (2), 304–315. doi:10.1016/j.brs.2021.01.018.

Belardinelli, P., Biabani, M., Blumberger, D.M., Bortoletto, M., Casarotto, S., David, O., et al., 2019. Reproducibility in TMS-EEG studies: a call for data sharing, standard procedures and effective experimental control. Brain Stimul. 12 (3), 787–790. doi:10.1016/j.brs.2019.01.010.

Belardinelli, P., Konig, F., Liang, C., Premoli, I., Desideri, D., Muller-Dahlhaus, F., et al., 2021. TMS-EEG signatures of glutamatergic neurotransmission in human cortex. Sci. Rep. 11 (1), 8159. doi:10.1038/s41598-021-87533-z.

Biabani, M., Fornito, A., Coxon, J.P., Fulcher, B.D., Rogasch, N.C., 2021. The correspondence between EMG and EEG measures of changes in cortical excitability following transcranial magnetic stimulation. J. Physiol. 599 (11), 2907–2932. doi:10.1113/JP280966.

Biabani, M., Fornito, A., Mutanen, T.P., Morrow, J., Rogasch, N.C., 2019. Characterizing and minimizing the contribution of sensory inputs to TMS-evoked potentials. Brain Stimul. 12 (6), 1537–1552. doi:10.1016/j.brs.2019.07.009.

Bonato, C., Miniussi, C., Rossini, P.M., 2006. Transcranial magnetic stimulation and cortical evoked potentials: a TMS/EEG co-registration study. Clin. Neurophysiol. 117 (8), 1699–1707. doi:10.1016/j.clinph.2006.05.006.

Burke, M.J., Kaptchuk, T.J., Pascual-Leone, A, 2019. Challenges of differential placebo effects in contemporary medicine: the example of brain stimulation. Ann. Neurol. 85 (1), 12–20. doi:10.1002/ana.25387.

Casali, A.G., Casarotto, S., Rosanova, M., Mariotti, M., Massimini, M., 2010. General indices to characterize the electrical response of the cerebral cortex to TMS. Neuroimage 49 (2), 1459–1468. doi:10.1016/j.neuroimage.2009.09.026.

Cash, R.F., Noda, Y., Zomorrodi, R., Radhu, N., Farzan, F., Rajji, T.K., et al., 2017. Characterization of Glutamatergic and GABAA-mediated neurotransmission in motor and dorsolateral prefrontal cortex using paired-pulse TMS-EEG. Neuropsychopharmacology 42 (2), 502–511. doi:10.1038/npp.2016.133.

Chung, S.W., Sullivan, C.M., Rogasch, N.C., Hoy, K.E., Bailey, N.W., Cash, R.F.H., et al., 2019. The effects of individualised intermittent theta burst stimulation in the prefrontal cortex: a TMS-EEG study. Hum. Brain Mapp. 40 (2), 608–627. doi:10.1002/hbm.24398.

Conde, V., Tomasevic, L., Akopian, I., Stanek, K., Saturnino, G.B., Thielscher, A., et al., 2019. The non-transcranial TMS-evoked potential is an inherent source of ambiguity in TMS-EEG studies. Neuroimage 185, 300–312. doi:10.1016/j.neuroimage.2018.10.052.

Counter, S.A., Borg, E., 1992. Analysis of the coil generated impulse noise in extracranial magnetic stimulation. Electroencephalogr. Clin. Neurophysiol. 85 (4), 280–288. doi:10.1016/0168-5597(92)90117-t.

Darmani, G., Ziemann, U., 2019. Pharmacophysiology of TMS-evoked EEG potentials: a mini-review. Brain Stimul. 12 (3), 829–831. doi:10.1016/j.brs.2019.02.021.

Du, X., Choa, F.S., Summerfelt, A., Rowland, L.M., Chiappelli, J., Kochunov, P., et al., 2017. N100 as a generic cortical electrophysiological marker based on decomposition of TMS-evoked potentials across five anatomic locations. Exp. Brain Res. 235 (1), 69–81. doi:10.1007/s00221-016-4773-7.

Esser, S.K., Huber, R., Massimini, M., Peterson, M.J., Ferrarelli, F., Tononi, G., 2006. A direct demonstration of cortical LTP in humans: a combined TMS/EEG study. Brain Res. Bull. 69 (1), 86–94. doi:10.1016/j.brainresbull.2005.11.003.

Fecchio, M., Pigorini, A., Comanducci, A., Sarasso, S., Casarotto, S., Premoli, I., et al., 2017. The spectral features of EEG responses to transcranial magnetic stimulation of the primary motor cortex depend on the amplitude of the motor evoked potentials. PLoS One 12 (9), e0184910. doi:10.1371/journal.pone.0184910.

Fernandez, L., Biabani, M., Do, M., Opie, G.M., Hill, A.T., Barham, M.P., et al., 2021. Assessing cerebellar-cortical connectivity using concurrent TMS-EEG: a feasibility study. J. Neurophysiol. doi:10.1152/jn.00617.2020.

Ferreri, F., Pasqualetti, P., Maatta, S., Ponzo, D., Ferrarelli, F., Tononi, G., et al., 2011. Human brain connectivity during single and paired pulse transcranial magnetic stimulation. Neuroimage 54 (1), 90–102. doi:10.1016/j.neuroimage.2010.07.056.

Freedberg, M., Reeves, J.A., Hussain, S.J., Zaghloul, K.A., Wassermann, E.M., 2020. Identifying site- and stimulation-specific TMS-evoked EEG potentials using a quantitative cosine similarity metric. PLoS One 15 (1), e0216185. doi:10.1371/journal.pone.0216185.

Fuggetta, G., Fiaschi, A., Manganotti, P., 2005. Modulation of cortical oscillatory activities induced by varying single-pulse transcranial magnetic stimulation intensity over the left primary motor area: a combined EEG and TMS study. Neuroimage 27 (4), 896–908. doi:10.1016/j.neuroimage.2005.05.013.

Gordon, P.C., Desideri, D., Belardinelli, P., Zrenner, C., Ziemann, U., 2018. Comparison of cortical EEG responses to realistic sham versus real TMS of human motor cortex. Brain Stimul. 11 (6), 1322–1330. doi:10.1016/j.brs.2018.08.003.

Gosseries, O., Sarasso, S., Casarotto, S., Boly, M., Schnakers, C., Napolitani, M., et al., 2015. On the cerebral origin of EEG responses to TMS: insights from severe cortical lesions. Brain Stimul. 8 (1), 142–149. doi:10.1016/j.brs.2014.10.008.

Groppa, S., Oliviero, A., Eisen, A., Quartarone, A., Cohen, L.G., Mall, V., et al., 2012. A practical guide to diagnostic transcranial magnetic stimulation: report of an IFCN committee. Clin. Neurophysiol. 123 (5), 858–882. doi:10.1016/j.clinph.2012.01.010.

Hallett, M., Di Iorio, R., Rossini, P.M., Park, J.E., Chen, R., Celnik, P., et al., 2017. Contribution of transcranial magnetic stimulation to assessment of brain connectivity and networks. Clin. Neurophysiol. 128 (11), 2125–2139. doi:10.1016/j.clinph.2017.08.007.

Hamalainen, M.S., Ilmoniemi, R.J., 1994. Interpreting magnetic fields of the brain: minimum norm estimates. Med. Biol. Eng. Comput. 32 (1), 35–42.

Harquel, S., Bacle, T., Beynel, L., Marendaz, C., Chauvin, A., David, O., 2016. Mapping dynamical properties of cortical microcircuits using robotized TMS and EEG: towards functional cytoarchitectonics. Neuroimage 135, 115–124. doi:10.1016/j.neuroimage.2016.05.009.

Herring, J.D., Thut, G., Jensen, O., Bergmann, T.O., 2015. Attention modulates TMS-locked alpha oscillations in the visual cortex. J. Neurosci. 35 (43), 14435–14447. doi:10.1523/JNEUROSCI.1833-15.2015.

Hill, A.T., Rogasch, N.C., Fitzgerald, P.B., Hoy, K.E., 2016. TMS-EEG: a window into the neurophysiological effects of transcranial electrical stimulation in non-motor brain regions. Neurosci. Biobehav. Rev. 64, 175–184. doi:10.1016/j.neubiorev.2016.03.006.

Ilmoniemi, R.J., Kicic, D., 2010. Methodology for combined TMS and EEG. Brain Topogr. 22 (4), 233–248. doi:10.1007/s10548-009-0123-4.

Ilmoniemi, R.J., Virtanen, J., Ruohonen, J., Karhu, J., Aronen, H.J., Naatanen, R., et al.,

1997. Neuronal responses to magnetic stimulation reveal cortical reactivity and connectivity. Neuroreport 8 (16), 3537–3540.
Kenemans, J.L., 2015. Specific proactive and generic reactive inhibition. Neurosci. Biobehav. Rev. 56, 115–126. doi:10.1016/j.neubiorev.2015.06.011.
Komssi, S., Kahkonen, S., 2006. The novelty value of the combined use of electroencephalography and transcranial magnetic stimulation for neuroscience research. Brain Res. Rev. 52 (1), 183–192. doi:10.1016/j.brainresrev.2006.01.008.
Komssi, S., Kahkonen, S., Ilmoniemi, R.J., 2004. The effect of stimulus intensity on brain responses evoked by transcranial magnetic stimulation. Hum. Brain Mapp. 21 (3), 154–164. doi:10.1002/hbm.10159.
Koponen, L.M., Goetz, S.M., Tucci, D.L., Peterchev, A.V., 2020. Sound comparison of seven TMS coils at matched stimulation strength. Brain Stimul. 13 (3), 873–880. doi:10.1016/j.brs.2020.03.004.
Lin, Y.Y., Shih, Y.H., Chen, J.T., Hsieh, J.C., Yeh, T.C., Liao, K.K., et al., 2003. Differential effects of stimulus intensity on peripheral and neuromagnetic cortical responses to median nerve stimulation. Neuroimage 20 (2), 909–917. doi:10.1016/S1053-8119(03)00387-2.
Lioumis, P., Kicic, D., Savolainen, P., Makela, J.P., Kahkonen, S., 2009. Reproducibility of TMS-Evoked EEG responses. Hum. Brain Mapp. 30 (4), 1387–1396. doi:10.1002/hbm.20608.
Massimini, M., Ferrarelli, F., Huber, R., Esser, S.K., Singh, H., Tononi, G., 2005. Breakdown of cortical effective connectivity during sleep. Science 309 (5744), 2228–2232. doi:10.1126/science.1117256.
Mennemeier, M., Triggs, W., Chelette, K., Woods, A., Kimbrell, T., Dornhoffer, J., 2009. Sham transcranial magnetic stimulation using electrical stimulation of the scalp. Brain Stimul. 2 (3), 168–173. doi:10.1016/j.brs.2009.02.002.
Nikouline, V., Ruohonen, J., Ilmoniemi, R.J., 1999. The role of the coil click in TMS assessed with simultaneous EEG. Clin. Neurophysiol. 110 (8), 1325–1328.
Nikulin, V.V., Kicic, D., Kahkonen, S., Ilmoniemi, R.J., 2003. Modulation of electroencephalographic responses to transcranial magnetic stimulation: evidence for changes in cortical excitability related to movement. Eur. J. Neurosci. 18 (5), 1206–1212. doi:10.1046/j.1460-9568.2003.02858.x.
Novembre, G., Pawar, V.M., Kilintari, M., Bufacchi, R.J., Guo, Y., Rothwell, J.C., et al., 2019. The effect of salient stimuli on neural oscillations, isometric force, and their coupling. Neuroimage 198, 221–230. doi:10.1016/j.neuroimage.2019.05.032.
Oostenveld, R., Fries, P., Maris, E., Schoffelen, J.M., 2011. FieldTrip: open source software for advanced analysis of MEG, EEG, and invasive electrophysiological data. Comput. Intell. Neurosci. 2011, 156869. doi:10.1155/2011/156869.
Opitz, A., Legon, W., Mueller, J., Barbour, A., Paulus, W., Tyler, W.J., 2014. Is sham cTBS real cTBS? The effect on EEG dynamics. Front. Hum. Neurosci. 8, 1043. doi:10.3389/fnhum.2014.01043.
Paus, T., Sipila, P.K., Strafella, A.P., 2001. Synchronization of neuronal activity in the human primary motor cortex by transcranial magnetic stimulation: an EEG study. J. Neurophysiol. 86 (4), 1983–1990. doi:10.1152/jn.2001.86.4.1983.
Premoli, I., Bergmann, T.O., Fecchio, M., Rosanova, M., Biondi, A., Belardinelli, P., et al., 2017. The impact of GABAergic drugs on TMS-induced brain oscillations in human motor cortex. Neuroimage 163, 1–12. doi:10.1016/j.neuroimage.2017.09.023.
Premoli, I., Castellanos, N., Rivolta, D., Belardinelli, P., Bajo, R., Zipser, C., et al., 2014. TMS-EEG signatures of GABAergic neurotransmission in the human cortex. J. Neurosci. 34 (16), 5603–5612. doi:10.1523/JNEUROSCI.5089-13.2014.
Raffin, E., Harquel, S., Passera, B., Chauvin, A., Bougerol, T., David, O, 2020. Probing regional cortical excitability via input-output properties using transcranial magnetic stimulation and electroencephalography coupling. Hum. Brain Mapp. 41 (10), 2741–2761. doi:10.1002/hbm.24975.
Razza, L.B., Moffa, A.H., Moreno, M.L., Carvalho, A.F., Padberg, F., Fregni, F., et al., 2018. A systematic review and meta-analysis on placebo response to repetitive transcranial magnetic stimulation for depression trials. Prog. Neuropsychopharmacol. Biol. Psychiatry 81, 105–113. doi:10.1016/j.pnpbp.2017.10.016.
Rocchi, L., Di Santo, A., Brown, K., Ibanez, J., Casula, E., Rawji, V., et al., 2021. Disentangling EEG responses to TMS due to cortical and peripheral activations. Brain Stimul. 14 (1), 4–18. doi:10.1016/j.brs.2020.10.011.
Rogasch, N.C., Fitzgerald, P.B., 2013. Assessing cortical network properties using TMS-EEG. Hum. Brain Mapp. 34 (7), 1652–1669. doi:10.1002/hbm.22016.
Rogasch, N.C., Thomson, R.H., Farzan, F., Fitzgibbon, B.M., Bailey, N.W., Hernandez-Pavon, J.C., et al., 2014. Removing artefacts from TMS-EEG recordings using independent component analysis: importance for assessing prefrontal and motor cortex network properties. Neuroimage 101, 425–439. doi:10.1016/j.neuroimage.2014.07.037.
Rosanova, M., Casali, A., Bellina, V., Resta, F., Mariotti, M., Massimini, M., 2009. Natural frequencies of human corticothalamic circuits. J. Neurosci. 29 (24), 7679–7685. doi:10.1523/JNEUROSCI.0445-09.2009.
Rossi, S., Ferro, M., Cincotta, M., Ulivelli, M., Bartalini, S., Miniussi, C., et al., 2007. A real electro-magnetic placebo (REMP) device for sham transcranial magnetic stimulation (TMS). Clin. Neurophysiol. 118 (3), 709–716. doi:10.1016/j.clinph.2006.11.005.
Ruddy, K.L., Woolley, D.G., Mantini, D., Balsters, J.H., Enz, N., Wenderoth, N., 2018. Improving the quality of combined EEG-TMS neural recordings: introducing the coil spacer. J. Neurosci. Methods 294, 34–39. doi:10.1016/j.jneumeth.2017.11.001.
Seeck, M., Koessler, L., Bast, T., Leijten, F., Michel, C., Baumgartner, C., et al., 2017. The standardized EEG electrode array of the IFCN. Clin. Neurophysiol. 128 (10), 2070–2077. doi:10.1016/j.clinph.2017.06.254.
Siebner, H.R., Conde, V., Tomasevic, L., Thielscher, A., Bergmann, T.O., 2019. Distilling the essence of TMS-evoked EEG potentials (TEPs): a call for securing mechanistic specificity and experimental rigor. Brain Stimul. 12 (4), 1051–1054. doi:10.1016/j.brs.2019.03.076.
Stenroos, M., Nummenmaa, A., 2016. Incorporating and compensating cerebrospinal fluid in surface-based forward models of magneto- and electroencephalography. PLoS One 11 (7), e0159595. doi:10.1371/journal.pone.0159595.
Stenroos, M., Sarvas, J., 2012. Bioelectromagnetic forward problem: isolated source approach revis(it)ed. Phys. Med. Biol. 57 (11), 3517–3535. doi:10.1088/0031-9155/57/11/3517.
ter Braack, E.M., de Vos, C.C., van Putten, M.J., 2015. Masking the auditory evoked potential in TMS-EEG: a comparison of various methods. Brain Topogr. 28 (3), 520–528. doi:10.1007/s10548-013-0312-z.
Torquati, K., Pizzella, V., Della Penna, S., Franciotti, R., Babiloni, C., Rossini, P.M., et al., 2002. Comparison between SI and SII responses as a function of stimulus intensity. Neuroreport 13 (6), 813–819. doi:10.1097/00001756-200205070-00016.
Tremblay, S., Rogasch, N.C., Premoli, I., Blumberger, D.M., Casarotto, S., Chen, R., et al., 2019. Clinical utility and prospective of TMS-EEG. Clin. Neurophysiol. 130 (5), 802–844. doi:10.1016/j.clinph.2019.01.001.
Wessel, J.R., Aron, A.R, 2017. On the Globality of motor suppression: unexpected events and their influence on behavior and cognition. Neuron 93 (2), 259–280. doi:10.1016/j.neuron.2016.12.013.